



# A facile synthesis of copper sulfides composite with lithium-storage properties



Xuxiang Wang<sup>a,1</sup>, Yunhui Wang<sup>b,1</sup>, Xue Li<sup>b,1</sup>, Bo Liu<sup>b</sup>, Jinbao Zhao<sup>a,b,\*</sup>

<sup>a</sup> College of Energy, Xiamen University, Xiamen, 361005, China

<sup>b</sup> State Key Laboratory of Physical Chemistry of Solid Surfaces, Collaborative Innovation Center of Chemistry for Energy Materials, College of Chemistry and Chemical Engineering, Xiamen University, Xiamen, 361005, China

## HIGHLIGHTS

- Copper sulfides can be simply synthesized by heating a mixture of copper and sulfur powders in different stoichiometries.
- The copper-excess copper sulfides electrodes show enhanced electrochemical performance.
- The critical factor for  $\text{Cu}_x\text{S}$  electrodes achieving high performance is that the ratio of Cu and S is greater than 2.

## ARTICLE INFO

### Article history:

Received 27 October 2014

Received in revised form

6 December 2014

Accepted 29 January 2015

Available online 29 January 2015

### Keywords:

Copper sulfides

Copper excess

Cycling stability

High rate performance

Lithium ion batteries

## ABSTRACT

Copper sulfides are synthesized by heating a mixture of copper and sulfur powders in different stoichiometries in N-methyl-2-pyrrolidinone (NMP) solvent. All the electrodes show excellent electrochemical performance, especially 'copper excess' copper sulfides electrodes. These electrodes can be charged and discharged at high rate, with good capacity retention. The electrochemical reaction mechanism of copper sulfides during discharge–charge process is investigated. It is most likely that all of S element in the copper excess electrode would transfer into a crystal of  $\text{Cu}_2\text{S}$  during charge–discharge cycles, which corresponded to a single electrochemical reaction and showed excellent cycling and rate performance. These encouraging results indicate that copper-excess copper sulfides could be a promising anode material for lithium batteries with high rate capability.

© 2015 Elsevier B.V. All rights reserved.

## 1. Introduction

The last two decades have witnessed the rapid growth of lithium ion battery technology and its market in energy storage and electron devices application [1–5]. The advantages of these lithium ion batteries, compared with other battery devices, are of high energy density, long cycling life, long shelf life, etc. Today it is generally realized and accepted that each battery type has its pros and cons, lithium ion batteries are not in the stage yet to replace all others, even they have the great potentials. To further expand their

market potentials, there has been strong incentive to develop low cost lithium-ion batteries with high-energy, high-power density and high-safety.

Amongst many compounds which have been studied as alternatives [6–10] to transition metal oxides that are commonly used in current lithium ion battery, copper sulfides of the molecular formula of  $\text{Cu}_x\text{S}$  stand out because of their good electrical conductivities, high theoretical capacity and flat discharge curves, for example, covellite  $\text{CuS}$  is a good conductor ( $10^{-3} \text{ S cm}^{-1}$ ) and possesses a high capacity ( $560 \text{ mA}\cdot\text{h}\cdot\text{g}^{-1}$ ) which is almost four times of that of commercial  $\text{Li}_4\text{Ti}_5\text{O}_{12}$  [11–13]. Copper sulfide is a common nomenclature of binary compounds composed of copper and sulfur. In fact, these two elements form a myriad of binary compounds with different stoichiometries, such as  $\text{Cu}_2\text{S}$ ,  $\text{Cu}_7\text{S}_4$ ,  $\text{Cu}_{1.85}\text{S}$ ,  $\text{Cu}_{1.96}\text{S}$  and  $\text{Cu}_2\text{S}$  [14,15]. The mechanism of copper sulfides reacting with lithium ions and electrons is different from that of transition metal oxides, rather than an insertion reaction, it is a

\* Corresponding author. State Key Laboratory of Physical Chemistry of Solid Surfaces, Collaborative Innovation Center of Chemistry for Energy Materials, College of Chemistry and Chemical Engineering, Xiamen University, Xiamen, 361005, China.

E-mail address: [jbzhao@xmu.edu.cn](mailto:jbzhao@xmu.edu.cn) (J. Zhao).

<sup>1</sup> X. X. Wang, Y. H. Wang and X. Li contributed equally to this work and share first authorship.

replacement reaction in which the final product is Cu and  $\text{Li}_2\text{S}$  [9,13,16,17]. The formation of lithium polysulfides causes severe capacity decay during charge/discharge cycles, because lithium polysulfides can dissolve into electrolytes and drift away from the electrode [13]. Many attempts have been made to improve its capacity retention [10,18–20].  $\text{Cu}_2\text{S}$  film obtained from direct hydrothermal growth on Cu foil reported by Ni et al. and highly ordered large-scale  $\text{Cu}_2\text{S}$  nanowire arrays grown onto the copper current collector reported by Lai et al. can lead to excellent cycling performance [21,22]. The intrigue electrochemical behavior of  $\text{Cu}_2\text{S}$  materials on Cu foil inspired us to investigate the relation between the material chemistry and its electrochemical properties, and to further improve their electrochemical performance as anode for lithium ion batteries.

It is well known that electrochemically the ‘copper-excess’ copper sulfides electrodes [10,18–26] exhibit significant differences to the ‘copper-deficient’ copper sulfides electrodes [9,13]. If the molar ratio of copper to sulfur in electrodes is greater than 2:1, they are designated as ‘copper-excess’ copper sulfides electrodes, otherwise, they are ‘copper deficient’ copper sulfides electrodes. We carried out systematic work in attempt to uncover the origin of these pronounced differences. We first synthesized copper sulfides compounds with different Cu/S stoichiometries. And the influence of current collector on copper sulfides electrochemical performance is also studied in this work. In general, these ‘copper excess’ electrodes showed excellent performance compared with ‘copper deficient’ electrodes. This may be related to the excess copper can immobilize the active sulfur element to some extent, and the related mechanism is revealed in further discussion.

## 2. Experimental

### 2.1. Preparation of electrodes

Copper sulfides ( $\text{Cu}_x\text{S}$ ) were synthesized from copper powder (20–30 nm) (Aladdin, US) and sulfur powder (China National Medicines Corporation Ltd.). Different molar ratios of copper and sulfur were mixed and dispersed in N-methyl-2-pyrrolidone (NMP), and heated at 100 °C for 0.5 h before solvent evaporation. The synthesized  $\text{Cu}_x\text{S}$  are designated as  $\text{Cu}_x\text{S}$  I ( $x = 1$ ) and  $\text{Cu}_x\text{S}$  II ( $x = 2$ ), respectively.

The preparation of copper sulfides electrodes were as follows: copper sulfides powder, acetylene black, and PVDF were mixed at weight ratio of 70:15:15 in NMP to form slurry. The resultant slurry was uniformly coated onto Cu or Al foils respectively and dried in a vacuum at 60 °C for 12 h. A typical copper sulfides mass loading is 2.0–4.0  $\text{mg cm}^{-2}$  on each electrode.

Among these electrodes prepared, the ones with  $\text{Cu}_x\text{S}$  (I, II) coated onto the copper foil are considered as ‘copper excess’ copper sulfides electrodes; those with  $\text{Cu}_x\text{S}$  (I, II) coated onto the aluminum foil, are ‘copper deficient’ copper sulfides electrodes.

### 2.2. Cell assembly and electrochemical measurements

The electrochemical properties of copper sulfides electrodes were tested in CR2016-type coin cells with copper sulfides as the working electrode and lithium foil as the counter electrode. Celgard 2325 was used as separator. These Li/ $\text{Cu}_x\text{S}$  cells were assembled in an argon-filled glove box. The electrolyte was prepared by adding 1 M lithium bis(trifluoromethanesulfonyl)imide (LiTFSI) salt into a mixture of 1,2-dimethoxyethane (DME) and 1,3-dioxolane (DOL) at 1:1 volume ratio. The cycling performance of Li/ $\text{Cu}_x\text{S}$  cells were measured by charging and discharging at constant currents on Battery Test System (Land, Wuhan, China).

The cyclic voltammetric (CV) measurement of these Li/ $\text{Cu}_x\text{S}$  cells

were performed using three-electrode cell configuration on CHI1030C Electrochemical Work-station (Chenghua, Shanghai, China) at a scan rate of 0.1  $\text{mV s}^{-1}$ . A lithium foil was used as the counter and reference electrode.

### 2.3. Structure characterization

The X-ray diffraction patterns of the synthesized  $\text{Cu}_x\text{S}$  were collected on a PanalyticalX’pert PRO with a Cu  $K\alpha$  radiation ( $\lambda \approx 1.5418 \text{ \AA}$ ). The operating voltage and current were 40 kV and 30 mA, respectively, with scanning step of 2.0°  $\text{min}^{-1}$ . In order to analyze the changes of the crystal structure during charge and discharge process, the Li/ $\text{Cu}_x\text{S}$  cells were disassembled in an argon-filled glove box at different charged and discharged states, the electrode active materials were peeled off from the Cu or Al foil collector for XRD testing. The active substances were sealed with polyimide film tape (Capton®) to prevent exposure to the air.

The X-ray photoelectron spectrum (XPS) measurement was performed on PHI Quantum 2000 Scanning ESCA Microprobe, using monochromatized Al  $K\alpha$  radiation ( $h\nu = 1486.60 \text{ eV}$ ) with anode voltage of 15 kV. The pass energy was 60 eV for the survey spectra and 20 eV for particular elements. The microstructure of the samples was examined with Hitachi S-4800 Scanning electron microscope.

## 3. Results and discussions

### 3.1. Characterization of copper sulfides materials

The morphologies and crystal phases of the synthesized copper sulfides powders are characterized by SEM and TEM, as shown in Fig. 1. SEM images (Fig. 1a and b) indicate that the particles of these two samples are both coral-like and made of needle-like nanoparticles and all these nanoparticles are about one micrometer long and several hundred nanometers wide, even though the particle sizes of each sample are different. The needles in sample  $\text{Cu}_x\text{S}$  I are little thinner than that in sample  $\text{Cu}_x\text{S}$  II. Another little difference

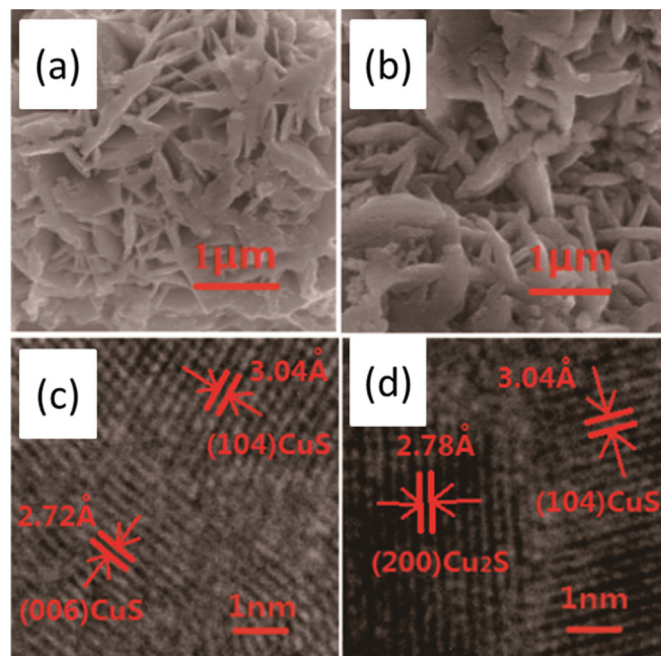


Fig. 1. SEM and TEM images of  $\text{Cu}_x\text{S}$ : (a, c)  $\text{Cu}_x\text{S}$  I, (b, d)  $\text{Cu}_x\text{S}$  II.

between these two samples is that the  $\text{Cu}_x\text{S}$  I has a more smooth than sample  $\text{Cu}_x\text{S}$  II.

The crystal phases of these samples from HRTEM studies illustrate their differences. Sample  $\text{Cu}_x\text{S}$  I (Fig. 1c) shows two lattice fringes with the lattice spacing of 3.04 Å and 2.72 Å, matching fairly well with {104} and {006} planes of CuS (JCPDS 001-1281), respectively; Sample  $\text{Cu}_x\text{S}$  II (Fig. 1d) shows several different kinds of lattice orientations, the interfringe spacing of 3.04 Å corresponds to {104} planes of CuS and the spacing of 2.78 Å matches with {200} planes of  $\text{Cu}_2\text{S}$  (JCPDS 003-1071).

XRD patterns of these three samples (Fig. 2) also confirm their structural and compositional difference.  $\text{Cu}_x\text{S}$  I (1:1) can be readily indexed to the hexagonal phase of CuS (JCPDS 001-1281) and no metallic copper peaks are observed significantly. The XRD pattern of  $\text{Cu}_x\text{S}$  II shows that it is a mixture: one set of the peaks is indexed to  $\text{Cu}_2\text{S}$  (JCPDS 003-1071); the set of peaks at  $2\theta = 43.3^\circ$ ,  $50.5^\circ$  and  $74.1^\circ$  belongs to the unreacted copper powders; and the set of peaks of  $48.1^\circ$  and the broad one at about  $32.0^\circ$  clearly marks the present of certain amount of CuS in it, which agrees well with that from HRTEM (Fig. 1d).

### 3.2. Electrochemical behaviors of the copper sulfides electrodes

Because we have found that enhanced electrochemical performance can be obtained for copper-excess electrodes, we also detect the typical discharge and charge features of these  $\text{Cu}_x\text{S}$  electrodes with copper or aluminum foils as current collectors. As shown in Fig. 3, these materials show similar electrochemical behaviors in their first few cycles. They all exhibit a small plateau around 1.9 V and a large plateau at 2.3 V in first charging step. The 2.3 V plateau keeps shrinking while 1.9 V plateau keeps increasing, and eventually the 2.3 V plateau is barely observable. Similar changes occur during discharge process. In the first discharge, each of the materials shows two voltage plateaus at around 2.0 V and 1.6 V. The lengths of these two plateaus depend heavily on the material itself with a small influence from current collectors. In  $\text{Cu}_x\text{S}$  I, the lengths of these two plateaus are roughly equal, but for  $\text{Cu}_x\text{S}$  II, the 2.0 V plateau is much smaller.

As cycling continued, the 2.0 V discharge plateaus for all materials keep shrinking while the 1.6 V plateaus keep increasing. The details about the capacity vs plateau (voltage) are listed in Table 1. The influence of different current collectors on cycling behaviors of the materials is worth of mentioning. The first noticeable difference is that in all cases, the capacities obtained with Cu foils are greater

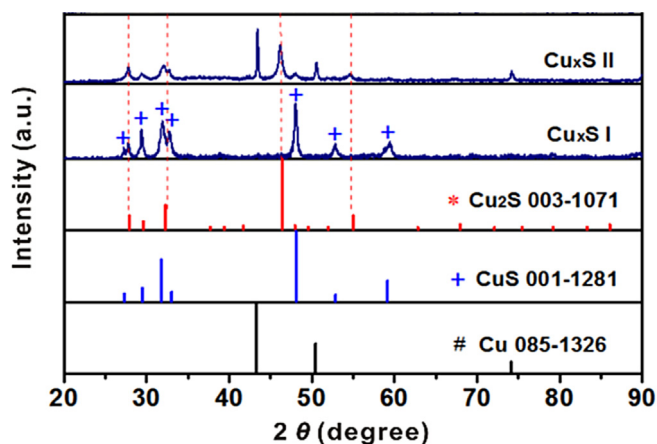


Fig. 2. XRD patterns of  $\text{Cu}_x\text{S}$  synthesized by different mole ratios of Cu and S. The bottom lines are the standard patterns of the  $\text{Cu}_2\text{S}$ , CuS and Cu.

than those on aluminum foils, especially for  $\text{Cu}_x\text{S}$  I. The active material in electrode with  $\text{Cu}_x\text{S}$  I coated on aluminum is CuS (from XRD data) and the electrode is considered as ‘copper-deficient’; even though the starting material in  $\text{Cu}_x\text{S}$  I coated on copper foil is also CuS, but CuS can readily reacts with copper to form ‘copper-excess’ compounds, thus the capacities of the ‘same’ materials are eventually quite different. The second noticeable difference is the voltage profile changes. In the case of aluminum foil, the 2.3 V charge plateau drops to 2.1 V but still can be seen after 100 cycles. Similar trends are also observed during discharge process in that the 2.0 V discharge plateaus are still observable after 100 cycles. However, neither of these features can be detected after 100 cycles in the case of copper foil as current collector. The third noticeable electrochemical difference is that the charge/discharge voltage gaps on aluminum are all comparatively larger than those on copper. Consequently, it further indicates the copper-excess electrodes are more superior due to the lower polarization and better reaction kinetics.

Galvanostatic cycle performance of these  $\text{Cu}_x\text{S}$  electrodes are shown in Fig. 4 and the detailed comparison is summarized in Table 2. By comparing the cycling stability of the electrodes on aluminum foils and on copper foils, it is obvious that  $\text{Cu}_x\text{S}$  II coated onto the copper current collector can achieve higher energy density, and better cycling stabilities. Hence, we decided to examine the electrochemical performance of  $\text{Cu}_x\text{S}$  II in more detail on copper foil. Its rate capability is shown in Fig. 5. The current rate increases from 1 C to 20 C, five cycles are recorded for each stepwise increment. Even at 20 C, the capacity obtained is  $210 \text{ mAh g}^{-1}$ , meaning about 67% capacity retention of 1 C discharge.

The insight of the change of  $\text{Cu}_x\text{S}$  in the electrochemical properties upon lithiation and delithiation can be gained by cyclic voltammetrical (CV) studies. The CV data of these  $\text{Cu}_x\text{S}$  electrodes are shown in Fig. 6. All these cyclic voltammograms are very complicate and indicate very complex electrochemical reaction mechanism, but the general features are quite similar. The  $\text{Cu}_x\text{S}$  I material (Fig. 6a and b) exhibits two redox couples in the first scan: two well-defined peaks at the voltage of around 2.0 V and 1.6 V while scanning cathodically, and two well-defined peaks at around 2.3 V and 1.9 V during anodic scan. The magnitudes of these peaks are quite different on different current collectors. Upon subsequent cycling, the cathodic peak at 2.0 V and anodic peak at around 2.3 V gradually decrease, and are eventually unobservable if copper used as current collector (Fig. 6b). All these CV results are highly consistent with the charge–discharge curves, and the mechanism of the electrochemical reactions will be discussed later.

All of the above-mentioned results indicate the copper-excess  $\text{Cu}_2\text{S}$  electrode, especially when coated on the copper current collector, has excellent electrochemical performance. In order to verify this assumption further, we have prepared copper sulfides with the molar ratio of copper and sulfur is 3:1 (hereafter referred to as  $\text{Cu}_x\text{S}$  III). And the XRD, SEM/TEM and electrochemical performance data is shown in Figs. S1–S4, respectively. As seen from the Figs. S1 and S2, the  $\text{Cu}_x\text{S}$  III is also coral-like and made of needle-like nanoparticles, and the crystal phase can be readily indexed into a pure copper phase and a  $\text{Cu}_2\text{S}$  phase (JCPDS 003-1071). This is understandable since the molar ratio of copper to sulfur is 3:1 in our starting materials. No peak belonged to CuS is observed. As shown in Fig. S3, the charge/discharge curves coincide much better than the  $\text{Cu}_x\text{S}$  I and  $\text{Cu}_x\text{S}$  II electrodes. In addition, the temporary voltage platform at 2.3 V disappears immediately after first cycle. These indicate the  $\text{Cu}_x\text{S}$  III exhibits higher electrochemical reversibility and more stable working voltage. And these properties are crucial to the practical application. We also compare the cycle stability with different current collectors, as shown in Fig. S4. The better

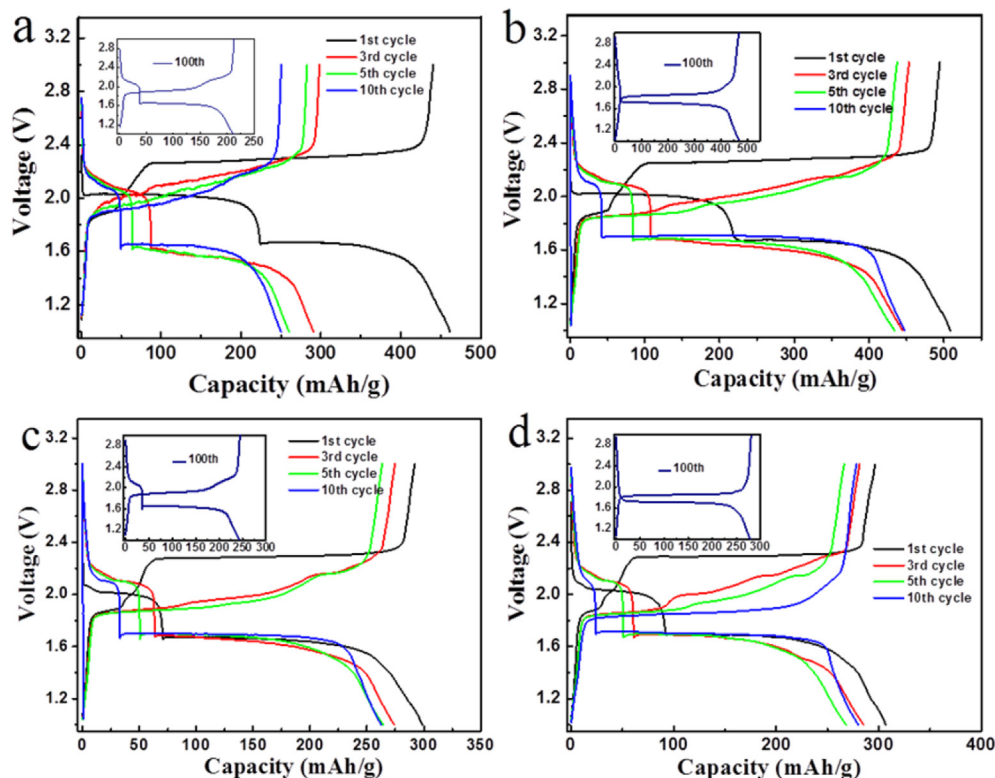


**Fig. 3.** Electrochemical performance of Li/Cu<sub>x</sub>S cells. Discharge–charge voltage profiles of (a, b) Cu<sub>x</sub>S I and (c, d) Cu<sub>x</sub>S II. The prepared active materials in the cells of (a, c) and (b, d) were coated to the aluminum foil and copper foil respectively. The figure inset presents the profile of the 100th cycle. The cells were tested between 1.0 and 3.0 V versus Li/Li<sup>+</sup> at a rate of 1.0 C (1 C = 1675 mA g<sup>-1</sup>).

stability can be obtained by using copper as the current collector, especially in the first few cycles.

### 3.3. Structural evolution of Cu<sub>x</sub>S I during cycling

In order to gain further insight into the electrochemical reaction mechanism, some structural characterizations have been done to detect the reaction process. Fig. 7 shows the SEM and HRTEM images of Cu<sub>x</sub>S I and Cu<sub>x</sub>S II electrode materials after cycled for 100 times. The particle is about 5 μm (Fig. 6a), and is much bigger than that before cycling. Its crystal phase is also different from that before cycling. There is only one lattice fringe with spacing of 2.78 Å corresponds to {200} planes of Cu<sub>2</sub>S (JCPDS 003-1071) (Fig. 6b). Recalling that in Fig. (1a and c), the particles are coral-like and its crystal phase is pure CuS (JCPDS001-1281). After cycled for 100 cycles, its morphology is changed from small particles to agglomerate of plates and its crystal phase changed from CuS to Cu<sub>2</sub>S. The similar change can be seen for the Cu<sub>x</sub>S II electrode (Fig. 7c and d), the morphology is tend to agglomerate but the crystal phase is pure Cu<sub>2</sub>S (JCPDS 003-1071) from beginning to end. In summary, we

**Table 1**

Discharge capacity of 1st cycle at the rate of 0.2 C. For the Cu<sub>x</sub>S (I, II) electrode, the less amount of CuS it contains, the smaller percentage of the higher plateau's capacity it has.

Sample	Current collector	Discharge capacity of 1st cycle (mA g <sup>-1</sup> )	Capacity of the higher plateau (mA g <sup>-1</sup> )/percentage	Capacity of the lower plateau (mA g <sup>-1</sup> )/percentage
Cu <sub>x</sub> S I	Al	461.5	222.3/48.4%	238.2/51.6%
Cu <sub>x</sub> S I	Cu	508.4	218.0/42.9%	190.0/57.1%
Cu <sub>x</sub> S II	Al	298.5	70.6/23.7%	227.9/76.3%
Cu <sub>x</sub> S II	Cu	306.8	92.8/30.2%	234.0/69.8%

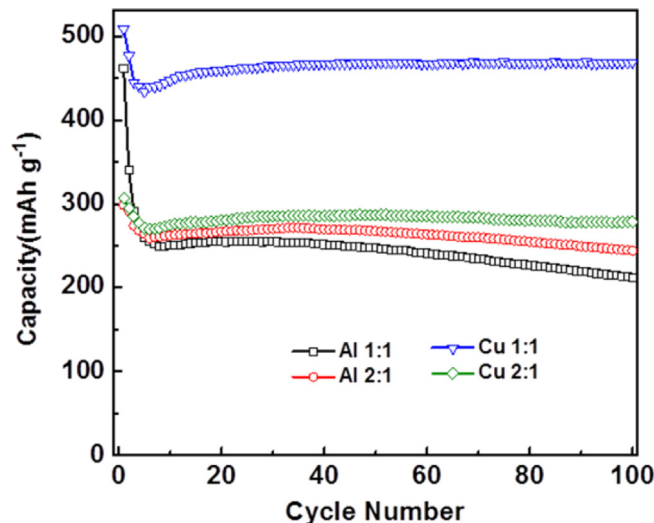


**Fig. 4.** Cycling performance of Cu<sub>x</sub>S I and Cu<sub>x</sub>S II at constant rate of 1.0 C, coated on the aluminum foil and the copper foil respectively.

**Table 2**

The capacities for Cu<sub>x</sub>S electrodes at discharge current rate of 1.0 C.

Sample	Current collector	Discharge capacity of 1st cycle (mA g <sup>-1</sup> )	Discharge capacity of 100 <sup>th</sup> cycle (mA g <sup>-1</sup> )	Capacity retention
Cu <sub>x</sub> S I	Al	461.5	212.1	46.0%
Cu <sub>x</sub> S I	Cu	508.4	468.8	92.2%
Cu <sub>x</sub> S II	Al	298.5	243.2	81.5%
Cu <sub>x</sub> S II	Cu	306.8	278.8	90.9%

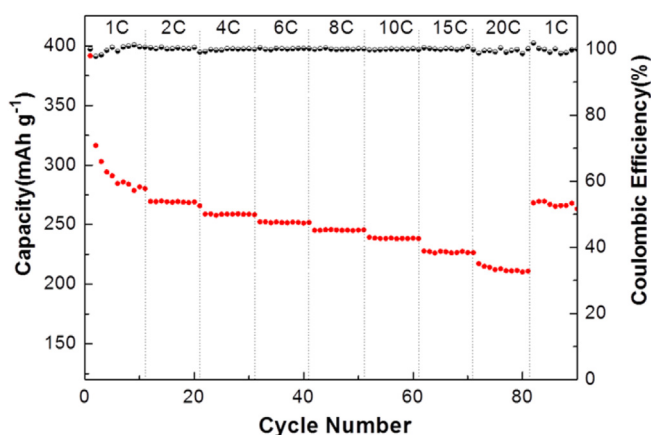


Fig. 5. Rate performance of  $\text{Cu}_x\text{S}$  II coated on the copper foil.

believe the composition of the  $\text{Cu}_x\text{S}$  electrode materials may be a major factor that governs the cycling life of copper sulfides in lithium ion cells.

To fully understand its structural evolution during cycling, quasi in-situ XRD characterizations are conducted on five  $\text{Cu}_x\text{S}$  I cycled samples (Fig. 8a). Before the XRD tests, these Li/ $\text{Cu}_x\text{S}$  I coin cells have been cycled galvanostatically at 0.5 C rate for 30 cycles, then are terminated the electrochemical discharge/charge process at different charged/discharged states, in accordance with the electrochemical plot shown in Fig. 8b.

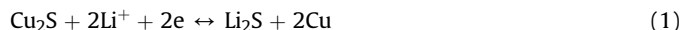
At a fully charged state (unlithiated, curve a), the XRD diagram shows well-defined peaks that could be associated with  $\text{Cu}_2\text{S}$  ( $27.9^\circ$ ,  $32.2^\circ$ ,  $46.3^\circ$ ,  $54.9^\circ$ ; JCPDS 003-1071). The XRD patterns of the fully discharged products (lithiated, curve c) could be associated with  $\text{Li}_2\text{S}$  ( $26.9^\circ$ ,  $31.2^\circ$ ,  $44.8^\circ$ ,  $53.1^\circ$ ; JCPDS 089-2838) and Cu ( $43.3^\circ$ ,  $50.4^\circ$ ,  $74.1^\circ$ ; JCPDS 01-089-2838). During the discharge process, the  $\text{Cu}_2\text{S}$  peaks decrease in intensity and disappear at the end of discharge reaction, while the peaks of  $\text{Li}_2\text{S}$  and Cu become prominent, indicating that  $\text{Cu}_2\text{S}$  is reduced to  $\text{Li}_2\text{S}$  and Cu by lithiation. Scrutinizing the XRD data in Fig. 8a, we can see that the diffraction peak at  $25^\circ$ – $30^\circ$  split into two peaks which are indexed to  $\text{Cu}_2\text{S}$  {100} and  $\text{Li}_2\text{S}$  {100} (curve b). This indicates there are two kinds of crystalline structures coexist when electrode is discharged in half way. This phenomena also observed in the charging process (Fig. 8a, curve d), indicating that  $\text{Li}_2\text{S}$  and Cu reacted electrochemically to form  $\text{Cu}_2\text{S}$  and the electrochemical reaction is quite reversible. Thus the delithiation/lithiation reaction of  $\text{Cu}_2\text{S}$  should be considered as a single electrochemical reaction:  $\text{Cu}_2\text{S} + \text{Li} \leftrightarrow \text{Li}_2\text{S} + \text{Cu}$ , characterized by two very flat voltage plateaus at 1.70 V and 1.85 V in the process of charging and discharging.

#### 3.4. Proposed charge–discharge mechanism

It is well known that copper sulfides are far more complex than its simple formulae and they often exist in a variety of phases mostly consisting of closed-packed arrays of sulfur atoms with Cu atoms distributed randomly throughout the interstices [27–30]. The bonding in copper sulfides could not be correctly described in terms of a simple oxidation state formalism because the Cu–S bonds are somewhat covalent rather than ionic in character with high degree of delocalization resulting in complicated electronic band structures. Although many textbooks [31] sign the mixed valence formula  $(\text{Cu}^+)_2(\text{Cu}^{2+})(\text{S}^{2-})_2$  to  $\text{CuS}$ , Folmer et al. and Goh et al. argued that the copper ions in all the copper sulfides are monovalent, and more appropriate formulae would be

$(\text{Cu}^+)_3(\text{S}^{2-})(\text{S}_2)^-$  for  $\text{CuS}$ ,  $(\text{Cu}^+)_2(\text{S}^{2-})$  for  $\text{Cu}_2\text{S}$ , and  $(\text{Cu}^+)(\text{S}_2)^-$  for  $\text{CuS}_2$ , respectively, based upon the strong evidence given by X-ray photoelectron spectroscopic data [32–35].

From XRD data, the copper sulfides compounds synthesized here are within two molar ratio boundaries of  $\text{Cu}_2\text{S}$  and  $\text{CuS}$ . Thus we shall discuss the electrochemical reactions of these two compounds in an attempt to understand the quite different electrochemical behaviors between the ‘copper-excess’ and ‘copper-deficient’ copper sulfides. The ‘copper-excess’ copper sulfides (referred to the molar ratio of the copper and sulfur is greater than 2:1,  $\text{Cu}_2\text{S}$ ) in which copper ions are considered as  $(\text{Cu}^+)_2$  and sulfur ions as  $(\text{S}^{2-})$ , based on arguments by Folmer and Goh, react electrochemically as following:



It can be simplified as:



The above reactions correspond to the lower discharge voltage plateau at around 1.6 V and charge voltage plateau at around 1.9 V. As discharging, when the lithium ions intercalate between the active sites of sulfur and drive out the highly-mobile copper cations, resulting in the formation of copper dendrites [9].

This process is reversible during charge and discharge processes, which is supported by the quasi in-situ XRD characterizations shown in Fig. 8. It is also illustrated that the cubic  $\text{Cu}_2\text{S}$  and  $\text{Li}_2\text{S}$  structures present exactly the same sulfur array, thus one can act as a template for the other in the next step, like registering a memory, to enable electrochemically lithium ions to substitute and be replaced by reversibly by copper ions [9,18]. This is the reasonable explanation for the ‘copper excess’ copper sulfides have excellent cycling and rate performance. In our experiments, the materials as shown in Fig. 3(d) are closest to the idealized ‘copper excess copper sulfides’ systems and achieve the best cycling performance.

For ‘copper-deficient’ copper sulfides electrode, i.e.  $\text{CuS}$ , which is considered to be  $(\text{Cu}^+)_3(\text{S}^{2-})(\text{S}_2)^-$ , the reactions are proposed as following:



This can be described in detail as:



During the discharge process,  $(\text{S}_2)^-$  of electrode active materials is reduced to  $\text{S}^{2-}$  ( $\text{Li}_2\text{S}$ ) then Cu (I) is reduced to Cu at the voltage plateaus of 2.10 V and 1.70 V respectively. The reverse reactions of reaction (4) and (5) occur at the voltage of 1.85 V and 2.15 V, respectively.

The actual systems are much more complex than the two ideal compounds discussed above.  $\text{Cu}_x\text{S}$  can be regarded as a mixture of  $\text{CuS}$  and  $\text{Cu}_2\text{S}$ . In fact, even in the ‘copper-excess’ system (Fig. 3c and d), there is still a small amount of  $\text{CuS}$  presented at the short discharge plateau of 2.10 V. In the case of ‘copper-excess’ copper sulfides, the ‘infinite’ amount of copper source supplied by the excess copper powder from synthesis or by the current collectors which involved into the electrochemical reactions during charging and/or discharging processes, ensure the gradual formation of  $\text{Cu}_2\text{S}$  during cycling. Eventually, only  $\text{Cu}_2\text{S}$  is present as copper sulfides (Fig. 8).

The present and quickly disappearing after first few cycles of the

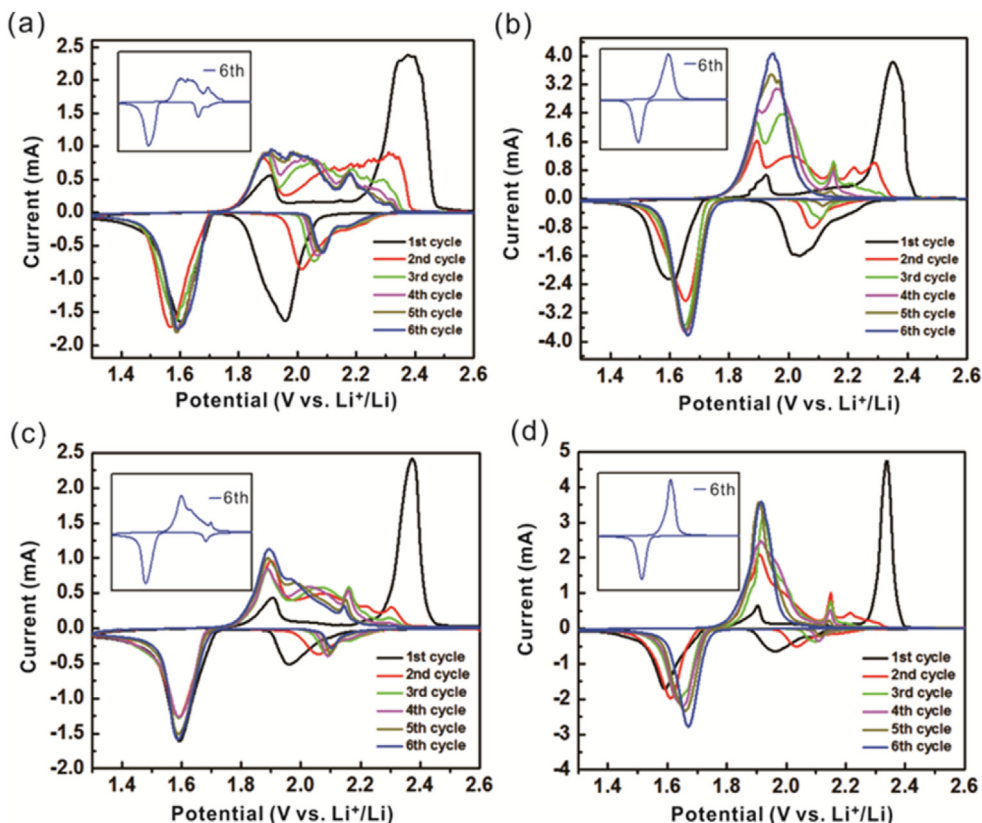


**Fig. 6.** Cyclic voltammetry curves of copper sulfides electrodes in the half-cells (Li/Cu<sub>x</sub>S) cycled between 1.3 and 2.6 V vs. Li/Li<sup>+</sup> at a rate of 0.1 mVs<sup>-1</sup>. (a, b) Cu<sub>x</sub>S I and (c, d) Cu<sub>x</sub>S II. The prepared active materials in the cells of (a, c) and (b, d) were coated onto the copper foil and aluminum foil respectively. The figure inset presents the CV curve of the 6th cycle.

high charge voltage plateau at 2.35 V in every sample is intriguing and its origin is still unclear. One possibility is that it is caused by a large Li<sub>2</sub>S overpotential (~1 V) because Li<sub>2</sub>S is usually considered to be electrochemically inactive due to its high electronic resistivity and low lithium ion diffusivity [36]. The gradual formation of polysulfides and new sulfur networks, especially the dendritic network of copper likely improves the conductivity and the lithium ion diffusivity of the electrode materials, and the electrochemical performance of the copper sulfides.

#### 4. Conclusions

In summary, we have demonstrated that the 'copper-excess' copper sulfides electrodes showed excellent cycling performance and rate capability. The excellent cycling and rate performance could be contributed to the high conductivity of copper sulfides and the unique displacement reaction between Cu<sub>2</sub>S and Li<sub>2</sub>S, both of them possess similar crystal structures. We believe and demonstrate that the most critical factor for achieving such good performances in Li-Cu<sub>x</sub>S batteries is that the amount of copper atoms in copper sulfides electrodes should exceed 2 times of the amount of sulfur atoms. (If the Cu film is selected as the current collector, the copper-rich condition can be built and the improved electrochemical performance can be obtained as well). When there is sufficient copper to react with sulfur, generating S<sub>x</sub><sup>2-</sup> species especially the (S<sub>2</sub>)<sup>-</sup> during the cycling is extremely inhibited, thereby preventing the capacity fading caused by S<sub>x</sub><sup>2-</sup> species dissolving into the electrolyte.

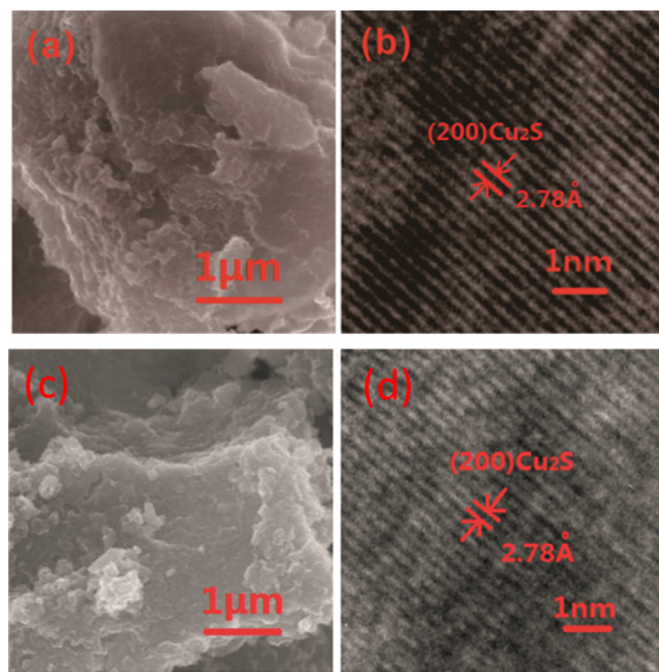


**Fig. 7.** (a) SEM and (b) TEM images of the copper sulfides electrodes which were collected from the Cu<sub>x</sub>S I electrodes using copper as current collector after 100 cycles. (c) SEM and (d) TEM images of the copper sulfides electrodes which were collected from the Cu<sub>x</sub>S II electrodes using copper as current collector after 100 cycles.

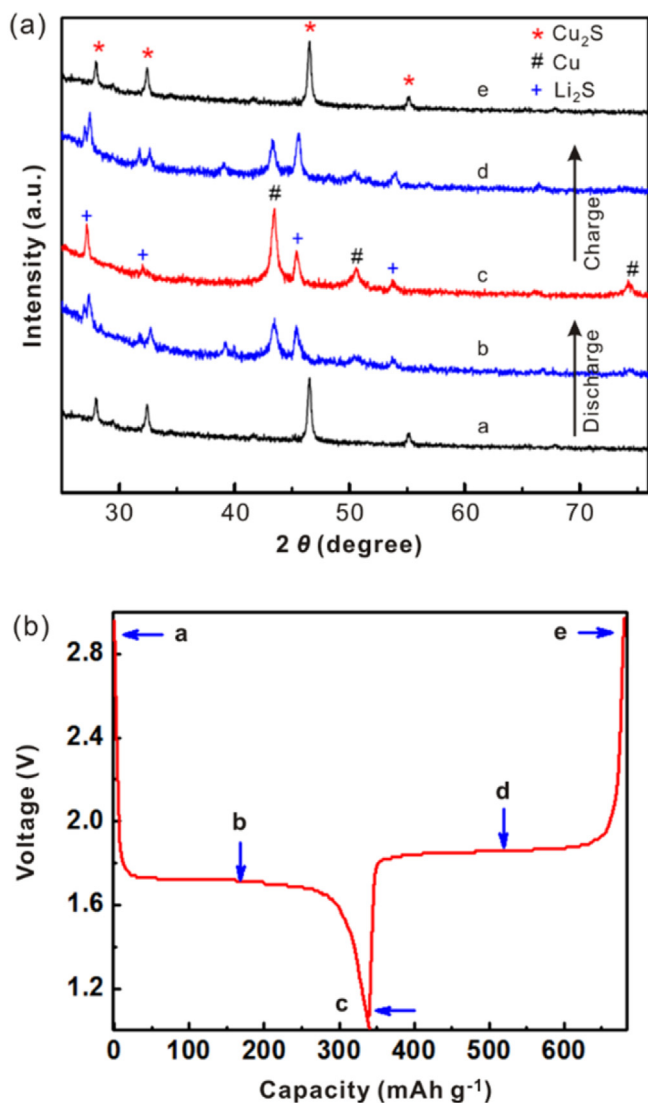


**Fig. 8.** (a) Quasi in situ XRD patterns of the  $\text{Cu}_x\text{S}$  I electrode using copper as current collector at different discharge/charge state: a) charged 100%, b) discharged 50%, c) discharged 100%, d) charged 50%, e) charged 100%. (b) The corresponding electrochemical plot during charge/discharge process at different state.

### Acknowledgment

This work was supported by grants from National Natural Science Foundation of China (21273185 and 21321062) and NFFTBS (J1310024). We thank Dr. Binbin Xu in Xiamen University for TEM test.

### Appendix A. Supplementary data

Supplementary data related to this article can be found at <http://dx.doi.org/10.1016/j.jpowsour.2015.01.172>.

### References

- [1] J.M. Tarascon, M. Armand, *Nature* 414 (2001) 359–367.
- [2] J.B. Goodenough, Y. Kim, *Chem. Mat.* 22 (2010) 587–603.
- [3] B. Scrosati, J. Hassoun, Y.K. Sun, *Energy Environ. Sci.* 4 (2011) 3287–3295.
- [4] A.S. Arico, P.G. Bruce, B. Scrosati, J.M. Tarascon, W.V. Schalkwijk, *Nat. Mater.* 4 (2005) 366–377.
- [5] M.M. Thackeray, C. Wolverton, E.D. Isaacs, *Energy Environ. Sci.* 5 (2012) 7854–7863.
- [6] P. Poizat, S. Laruelle, S. Grugeon, J.M. Tarascon, *J. Electrochem. Soc.* 149 (2002) A1212–A1217.
- [7] L.A. Montoro, J.M. Rosolen, J.H. Shin, S. Passerini, *Electrochim. Acta* 49 (2004) 3419–3429.
- [8] N.H. Idris, M.M. Rahman, S.L. Chou, J.Z. Wanga, D. Wexlerc, H.K. Liu, *Electrochimica. Acta* 58 (2011) 456–462.
- [9] A. Débart, L. Dupont, R. Patrice, J.M. Tarascon, *Solid State Sci.* 8 (2006) 640–651.
- [10] Y.R. Wang, X.W. Zhang, P. Chen, H.T. Liao, S.Q. Cheng, *Electrochim. Acta* 80 (2012) 264–268.
- [11] K. Okamoto, S. Kawai, *Jpn. J. Appl. Phys.* 12 (1973) 1130–1138.
- [12] A. Etienne, *J. Electrochem. Soc.* 117 (1970) 870–874.
- [13] J.S. Chung, H.J. Sohn, *J. Power Sources* 108 (2002) 226–231.
- [14] X. Jiang, Y. Xie, J. Lu, W. He, L. Zhu, Y. Qian, *J. Mater. Chem.* 10 (2000) 2193–2196.
- [15] P. Kumar, R. Nagarajan, *Inorg. Chem.* 50 (2011) 9204–9206.
- [16] G. Eichinger, H.P. Fritz, *Electrochim. Acta* 20 (1975) 753–757.
- [17] N. Yamakawa, M. Jiang, C.P. Grey, *J. Chem. Mater.* 21 (2009) 3162–3176.
- [18] B. Jache, B. Mogwitz, F. Klein, P. Adelhelm, *J. Power Sources* 247 (2014) 703–711.
- [19] F. Han, W.C. Li, D. Li, A.H. Lu, *ChemelectroChem.* 1 (2014) 733–740.
- [20] C.H. Feng, L. Zhang, Z.H. Wang, X.Y. Song, K.N. Sun, F. Wu, G. Liu, *J. Power Sources* 269 (2014) 550–555.
- [21] S.B. Ni, T. Li, X.L. Yang, *Electrochim. Acta* 91 (2013) 267–274.
- [22] C.H. Lai, K.W. Huang, J.H. Cheng, C.Y. Lee, B.J. Hwang, L.J. Chen, *J. Mater. Chem.* 20 (2010) 6638–6645.
- [23] Y. Han, Y.P. Wang, W.H. Gao, Y.J. Wang, L.F. Jiao, H.T. Yuan, S.X. Liu, *Powder Technol.* 212 (2011) 64–68.
- [24] Y.H. Chen, C. Davoisne, J.M. Tarascon, C. Guéry, *J. Mater. Chem.* 22 (2012) 5295–5299.
- [25] R. Cai, J. Chen, J.X. Zhu, C. Xu, W.Y. Zhang, C.M. Zhang, W.H. Shi, H.T. Tan, D. Yang, H.H. Hng, T.M. Lim, Q.Y. Yan, *J. Phys. Chem. C* 116 (2012) 12468–12474.
- [26] A. Hayashi, T. Ohtomo, F. Mizuno, K. Tadanaga, M. Tatsumisago, *Electrochem. Commun.* 5 (2003) 701–705.
- [27] R. Sadanaga, M. Ohmasa, N. Morimoto, *J. Miner.* 5 (1965) 275–279.
- [28] N. Morimoto, G. Kullerud, *Am. Mineral.* 48 (1963) 110–123.
- [29] M.J. Buerger, N.W. Buerger, *Am. Mineral.* 29 (1944) 55–71.
- [30] W.P. Lim, H.Y. Low, W.S. Chin, *Cryst. Growth Des.* 4 (2007) 2429–2435.
- [31] N.N. Greenwood, A. Earnshaw, *Chemistry of the Elements*, second ed., Butterworth-Heinemann, Oxford, 1997, p. 1181.
- [32] I. Nakai, Y. Sugitani, K. Nagashima, Y. Niwa, *J. Inorg. Nucl. Chem.* 40 (1978) 789–791.
- [33] J.C.W. Folmer, F. Jellinek, *J. Less Common Metals* 76 (1980) 153–162.
- [34] J.C.W. Folmer, F. Jellinek, G.H.M. Calis, *J. Solid State Chem.* 72 (1988) 137–144.
- [35] S.W. Goh, A.N. Buckley, R.N. Lamb, *Min. Eng.* 19 (2006) 204–208.
- [36] Y. Yang, G.Y. Zheng, S. Misra, J. Nelson, M.F. Toney, Y. Cui, *J. Am. Chem. Soc.* 134 (2012) 15387–15394.